17

Global Flood Partnership*

Lorenzo Alfieri[1,14], Sagy Cohen[2], John Galantowicz[3], Guy J.-P. Schumann[4,5], Mark A. Trigg[6], Ervin Zsoter[7], Christel Prudhomme[7,8,9], Andrew Kruczkiewicz[10,11], Erin Coughlan de Perez[10,11,12], Zachary Flamig[13], Roberto Rudari[14], Huan Wu[15,16,17], Robert F. Adler[18], Robert G. Brakenridge[19], Albert Kettner[19], Albrecht Weerts[20,21], Patrick Matgen[22], Saiful A.K.M. Islam[23], Tom de Groeve[1], Francesco Dottori[1], and Peter Salamon[1]

ABSTRACT

Every year riverine flooding affects millions of people in developing countries, due to the large population exposure in the floodplains and the lack of adequate flood protection. Preparedness and monitoring are effective ways to reduce flood risk. State-of-the-art technologies relying on satellite remote sensing as well as numerical hydrological and meteorological predictions can detect and monitor severe flood events at the global scale. This chapter describes the emerging role of the Global Flood Partnership (GFP), a global network of scientists, users, and private and public organizations active in global flood risk management. Currently, a number of GFP partner institutes regularly share results from their experimental products, developed to predict and monitor where and when flooding is taking place in near real time. Products of the GFP have already been used on several occasions by national environmental agencies and humanitarian organizations to support emergency operations and to reduce the overall socioeconomic impacts of disasters. The chapter includes a discussion on existing challenges and ways forward to improve rapid access to flood information and increase resilience to flooding.

[1] *Disaster Risk Management Unit, European Commission Joint Research Centre, Ispra, Italy*

[2] *Department of Geography, University of Alabama, Tuscaloosa, Alabama, USA*

[3] *Atmospheric and Environmental Research Inc., Lexington, Massachusetts, USA*

[4] *School of Geographical Sciences, University of Bristol, Bristol, United Kingdom*

[5] *Institute of Arctic and Alpine Research, University of Colorado, Boulder, Colorado, USA*

[6] *School of Civil Engineering, University of Leeds, Leeds, United Kingdom*

[7] *European Centre for Medium-range Weather Forecasts, Reading, United Kingdom*

[8] *Centre for Ecology and Hydrology, Wallingford, United Kingdom*

[9] *Department of Geography and Environment, Loughborough University, Loughborough, United Kingdom*

[10] *International Research Institute for Climate and Society, The Earth Institute, Columbia University, Palisades, New York, USA*

[11] *Red Cross Red Crescent Climate Centre, The Hague, The Netherlands*

[12] *Vrije Universiteit Amsterdam, Amsterdam, The Netherlands*

[13] *Center for Data Intensive Science, University of Chicago, Illinois, USA*

[14] *CIMA Research Foundation, Savona, Italy*

[15] *School of Atmospheric Sciences, Sun Yat-sen University, Guangdong, China*

[16] *Southern Marine Science and Engineering Laboratory, Guangdong, China*

[17] *Earth System Science Interdisciplinary Center, University of Maryland, College Park, Maryland, USA*

[18] *NASA Goddard Space Flight Center, Greenbelt, Maryland, USA*

[19] *Institute of Arctic and Alpine Research, University of Colorado, Boulder, Colorado, USA*

[20] *Deltares, Delft, The Netherlands*

[21] *Wageningen University and Research Centre, Wageningen, The Netherlands*

[22] *Luxembourg Institute of Science and Technology, Esch-sur-Alzette, Luxembourg*

[23] *Institute of Water and Flood Management, Bangladesh University of Engineering and Technology, Dhaka, Bangladesh*

**Adapted from Alfieri, L., Cohen, S., Galantowicz, J., Schumann, G.J.-P., Trigg, M.A., Zsoter, E., Prudhomme, C., Kruczkiewicz, A., Coughlan de Perez, E., Flamig, Z., Rudari, R., Wu, H., Adler, R.F., Brakenridge, R.G., Kettner, A., Weerts, A., Matgen, P., Islam, S.A.K.M., de Groeve, T., & Salamon, P. (2018). A global network for operational flood risk reduction.* Environmental Science and Policy, 84, *149–158. doi:10.1016/j.envsci.2018.03.014*

Global Drought and Flood: Observation, Modeling, and Prediction, Geophysical Monograph 265, First Edition.
Edited by Huan Wu, Dennis P. Lettenmaier, Qiuhong Tang, and Philip J. Ward.

DOI 10.1002/9781119427339.ch17

17.1. INTRODUCTION

Riverine flooding affects the vast majority of the world's regions. Flood risk has considerable spatial variability, due to heterogeneous natural processes, varied exposure and vulnerability to flooding, and to each country's or region's investment in flood preparedness and mitigation. Alfieri et al. (2017) estimated that combined flood losses in Asia and Africa account for 95% of people annually affected by floods globally and 73% of the total direct economic damage. While flash floods often result in higher average mortality rates, flooding from large rivers is responsible for the majority of people affected by floods every year, due to the vast extent of flood prone areas in populated regions (Jonkman, 2005; Pesaresi et al., 2017).

Satellite technologies have progressively changed the way to cope with large-scale floods throughout the entire disaster management cycle, from the preparedness to the recovery phase. Numerical weather predictions (NWP) have dramatically benefited from satellite data to improve forecast skill over the oceans, in areas poorly covered by conventional measurement networks, and to extend their predictability in time and for extreme events (Bouttier & Kelly, 2001). In addition, different sensors mounted on satellites have shown strong potential in detecting and monitoring surface water extent (Pekel et al., 2016), river and lake surface height (Alsdorf et al., 2007; Calmant et al., 2008), and large-scale flooding (Smith, 1997).

Such a wealth of data available in near real time has prompted research groups from many institutions worldwide to develop methods for flood prediction and monitoring at large scales. The potential benefits of these new products include a large variety of new applications for improved disaster preparedness and response. However, an immediate consequence is the need to (a) adapt experimental scientific tools for operational emergency activities, and (b) identify the limits of applicability of each tool and its outputs. To this end, the Global Flood Partnership (GFP;and https://gfp.jrc.ec.europa.eu) was established as an open international group of academics, research institutes, practitioners, public and private organizations active in the field of flood risk and emergency management. The goal is to foster the dialogue between scientists and users, whereby (a) scientists adapt their systems to the needs of emergency managers, and (b) emergency managers adapt and adjust existing workflows to include new systems and data. Currently, the GFP includes more than 450 members from six continents, registered through a dedicated mailing list. More than 100 organizations were represented during the first eight annual meetings, which have been held since 2011, while special sessions and side events are regularly held at relevant conferences throughout the year.

De Groeve et al. (2015) described the launch of the GFP with the aim to improve future flood management worldwide. Since then the GFP has received increasing attention by engaging more partners, sharing flood products, and through its designation in 2016 as a participating organization in the Group on Earth Observations (http://earthobservations.org).

This chapter illustrates the value of the GFP in supporting flood risk management for large-scale disasters by providing access to flood information and working towards closing the gap between availability and use of the information. It also shows how a suite of various products and expert knowledge can work in synergy to provide key information at different stages, before, during, and after severe floods.

"GFP activations" consist in the sharing of data and model results related to a specific upcoming or ongoing flood event through the GFP mailing list, which reaches all GFP members. Activation is commonly requested by partner institutes that are involved in the development of early warning systems, by organizations active in emergency operations, and by end users responding to the severe events. Two relevant examples of GFP activation for large-scale disasters are described in sections 17.3, showing how the GFP was crucial in assisting operational flood risk management and emergency operations. In the following section, models and products contributing to the GFP are grouped and described based on their timing of availability and the type of information they provide (Figure 17.1). In addition, several examples of GFP products available for operational flood risk reduction are provided in Table 17.1.

17.2. MODELS AND PRODUCTS

17.2.1. Early Warning Systems

Early warning systems (EWS) are designed to predict natural disasters before these occur. They are normally operated at large scales, with updating cycles in the order of hours to days, and variable levels of complexity including purely statistical processing, geophysical modeling, and forecast-based impact and cost-benefit assessments (see, e.g., Emerton et al., 2016). The EWS have a crucial role in the disaster risk management cycle as they can trigger flood preparedness actions by humanitarian organizations, emergency responders, and end users in potentially affected areas. Likewise, EWS can activate the flood management cycle within the GFP, and prompt further analysis and products from other member institutes.

An important element of the evaluation of EWS is defining how these will be deemed to be effective, keeping in mind their ultimate goal to provide insight to the potential socioeconomic impacts of disasters. The trigger to activate flood preparedness varies from system to system, though it is normally defined by a set of specific criteria, including a predicted variable (e.g., event

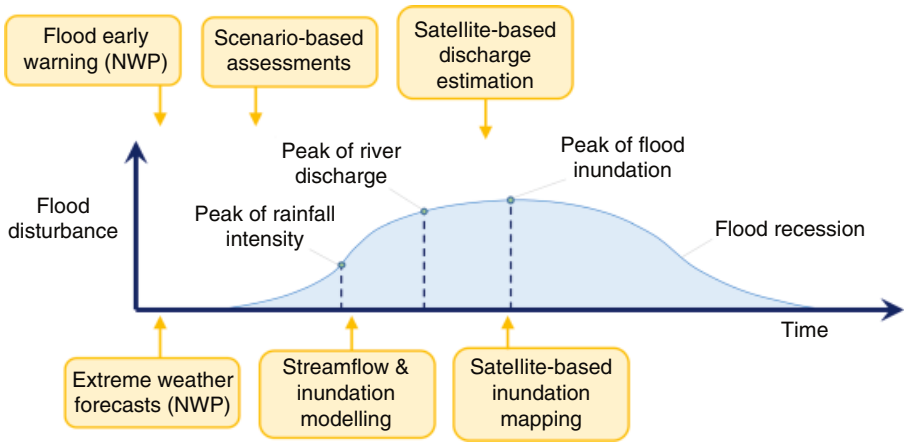

Figure 17.1 Timeline of a river flood and GFP product types to support disaster risk reduction before and during the event.

Table 17.1 A Nonexhaustive List of GFP Flood Products Regularly Updated on the Web, Grouped by Category

Category	Name	Predicted or measured variable	Maximum lead time (> 0) or latency (< 0)	References
Early warning systems	EFI, SOT	Extremes of rainfall, wind, temperature	15 days	www.ecmwf.int, Lalaurette (2003), Zsoter et al. (2015)
	GloFAS	Discharge, flood occurrence	15–30 days	www.globalfloods.eu, Alfieri et al. (2013), Hirpa et al. (2016)
	GLOFFIS, GLOSSIS	Floods, storm surges	10 days	globalfloodforecast.com
Scenario analysis	Inundation maps (modeled)	Flood depth and extent	NA	data.jrc.ec.europa.eu/collection/floods, Dottori et al. (2016), Pappenberger et al. (2012), Sampson et al. (2015), UNISDR (2015), Ward et al. (2013), Yamazaki et al. (2011)
	Inundation maps (satellite)	Flood extent	NA	floodobservatory.colorado.edu
Hydrological modeling	GFMS	Discharge, flood occurrence	5 days	flood.umd.edu, Wu et al. (2012)
	Floods.Global	Discharge	3 days	floods.global
Monitoring	River Watch	Discharge	−2 days	floodobservatory.colorado.edu/DischargeAccess.html
	NASA NRT-GFM	Flood extent	−1 day	floodmap.gsfc.nasa.gov, floodobservatory.colorado.edu, Brakenridge et al. (2017)
	FloodScan	Flood extent	−1 day	product.aer.com/index.php/floodscan
	GloFIMR	Flood extent	Available upon request	sdml.ua.edu/glofimr
	GDACS	Multihazard	−1 day	www.gdacs.org

frequency, peak discharge, river level, potential impact), lead-time to the event start/peak, forecast persistence (i.e., the agreement of consecutive forecasts), size of the river basin and probability, uncertainty or confidence of the forecast, amongst others. The skill of EWS triggers must be evaluated continuously, to optimize the tradeoff between correct predictions, false alarms, and missed events. An explanatory example of a trigger is that of the Flash Flood Notifications used in the European Flood Awareness System (EFAS; https://www.efas.eu; Raynaud et al., 2015; Thielen et al., 2009):

> "Notifications are issued when the probability of exceeding a 20 year return period (magnitude) of the surface runoff index (predicted variable) is forecasted to be larger than 35% (probability) and the forecasted start of the event is < 72 hours (lead time) in a region for which an EFAS partner exists (location)."

The EWS for weather-related disasters use NWP as their main dynamic input. These inputs can be in the form of deterministic predictions, allowing higher temporal and spatial resolution, or ensemble NWP, especially in the medium range, to assess the confidence of the forecasts (Adams & Pagano, 2016; Molteni et al., 1996). The EWS can be further classified into (a) extreme weather forecasts (EWF) and (b) flood early warning systems (FEWS), depending on the system complexity and on the variable used for flood prediction.

Extreme Weather Forecasts

Extreme weather forecasts are designed to estimate the extremeness of NWP through relatively simplified algorithms, thus informing about the possible occurrence of natural disasters. For instance, flash floods and riverine floods in temperate and tropical climates can be linked to extreme rainfall accumulations predicted within the forecast range. The extremeness of the event is estimated by comparing the predicted cumulated rainfall with its long-term statistical distribution, taken from a hindcast data set or from observed records, to estimate a probability of recurrence in a given year or season.

GFP Products The main GFP product included in this category is the Extreme Forecast Index (EFI; Lalaurette, 2003; Zsoter et al., 2015), which together with the Shift of Tail (SOT; Zsoter, 2006) index can detect significant deviations of the probability distribution of forecasts from the model climatology. The European Centre for Medium-range Weather Forecasts (ECMWF) produces operationally the EFI and SOT index of rainfall, wind, and temperature over various time ranges using their 51-member ensemble prediction system up to 15 days ahead (see example in Figure 17.2).

Complementary information for early detection of flooding through NWP include cyclone-track maps, probability of accumulated rainfall amounts, as well as large-scale anomaly indexes such as the El Niño/La Niña–Southern Oscillation. These products are requested by "user" organizations within the GFP in order to support decision-making. Decisions could include, for example, where and when certain actions should be taken to decrease impacts for a potential disaster, such as the allocation of medical resources and the prepositioning of response vehicles and personnel.

Flood Early Warning Systems

Systems included in FEWS distinguish themselves from EWF by the following:

- The use of a hydrological rather than a meteorological variable as a predictor for flooding (discharge or water level), which is usually estimated with hydrological models using NWP as input.
- The detection algorithm of extreme events keeps a memory of past conditions to initialize new forecasts, instead of computing an event magnitude based only on forecast values, as in extreme weather forecasts. Hence, the event peak, timing, and recession can be predicted over subsequent forecasts, including when the event is ongoing.

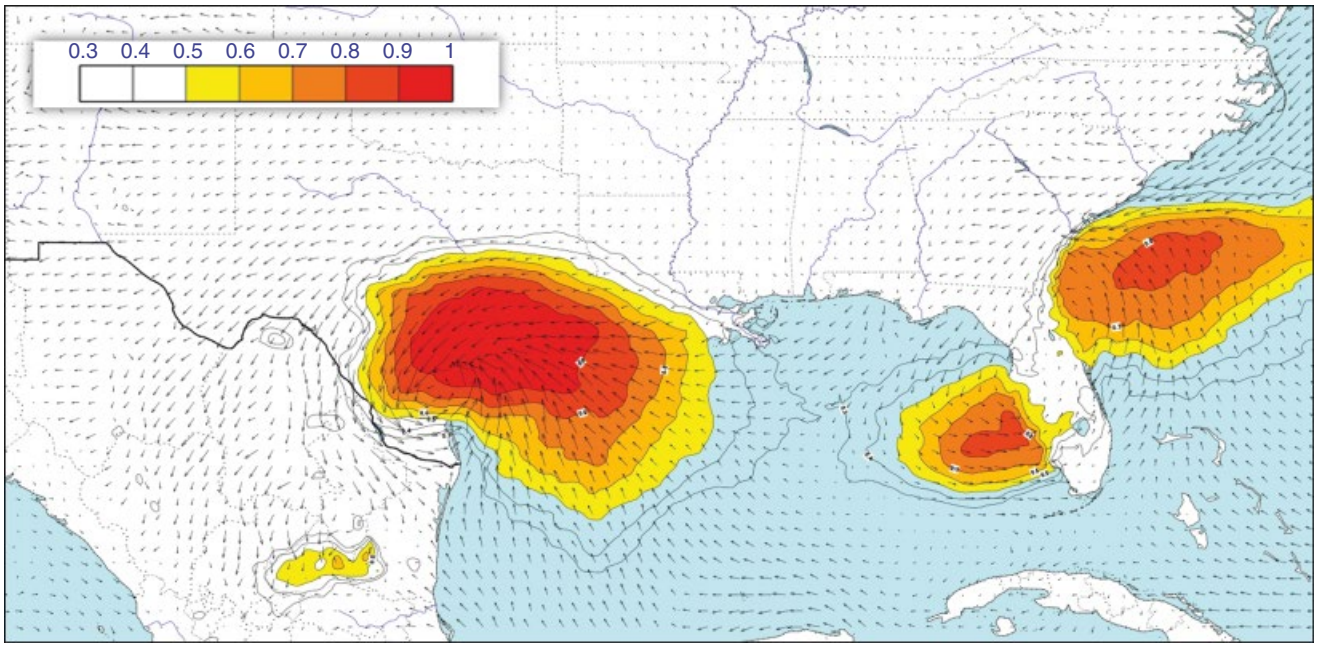

Figure 17.2 The EFI of 48 h accumulated precipitation for 26–27 August 2017 during the landfall of Tropical Storm Harvey in southern Texas, based on ECMWF ensemble forecasts of 25 August 2017, 1200 UTC. 10 m wind fields are also shown with arrows.

• Information on exposure and vulnerability of population and assets can be coupled to the hazard prediction to target the detection of extreme events in areas where the potential impacts are larger.

GFP Products In recent years a number of GFP activations were triggered by GloFAS, the Global Flood Awareness System (http://www.globalfloods.eu; Alfieri et al., 2013; Hirpa et al., 2016), developed jointly by the Joint Research Centre (JRC) of the European Commission and the ECMWF. The GloFAS gives an overview of upcoming floods in large river basins of the world with a forecast range up to 30 days. It is based on distributed hydrological simulation of ensemble NWP with global coverage. Streamflow forecasts are compared statistically to climatological simulations to detect areas with significant probability of exceeding flood-warning thresholds and the corresponding event magnitude.

17.2.2. Scenario Analysis

Following a GFP activation, the first products to become available are scenario analyses, which are assessments of potentially inundated areas corresponding to the event magnitude predicted by the EWS. Scenario analysis in nongauged regions can be produced with (a) inundation models and (b) satellite imagery.

Inundation Models

Inundation models are one-dimensional or two-dimensional hydraulic models that take a set of initial and boundary conditions (e.g., initial river stage, sea-level variations at the river mouth) and simulate the routing and spreading of a flood hydrograph through river channels and over their floodplains represented by a digital elevation model (DEM). Flood simulations are usually performed at higher spatial and temporal resolution than that used in the hydrological models used within EWS (Figure 17.3), at the expense of increasing computing resources. Therefore, detailed flood simulations must be constrained to specific river reaches where severe events are predicted to take place.

Real-time inundation maps can be produced by forcing the hydraulic model with flood hydrographs predicted by the EWS, to estimate areas likely to be inundated by the upcoming event. However, it is often preferred to use precomputed inundation maps derived from synthetic hydrographs with a range of recurrence intervals, resulting in a catalogue of events that can be used to estimate an inundation comparable to that of the predicted event (Dottori et al., 2017). The advantages of the latter option are: (a) prompt availability of maps for any river basin and for a range of flood magnitudes; (b) higher quality of precomputed maps which are often produced with calibrated input, while predicted hydrographs are more prone to quantitative errors.

GFP Products A number of GFP partners have already produced global inundation maps for a range of given flood return periods (Dottori et al., 2016; Pappenberger et al., 2012; Sampson et al., 2015; UNISDR, 2015; Ward et al., 2013; Yamazaki et al., 2011). These maps have been produced using various methods and spatial resolutions around 1 km, with some notable exceptions at 90 m (Sampson et al., 2015). Some of these maps and the underlying global flood models are included in an intercomparison and validation project carried out under the GFP umbrella (Bernhofer et al., 2018; Trigg et al., 2016).

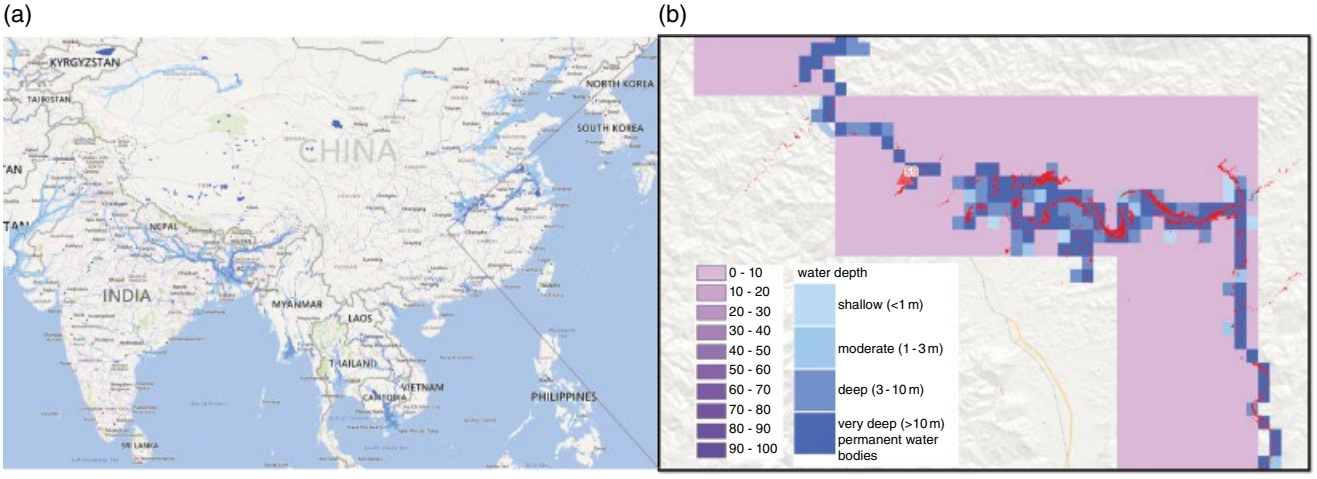

Figure 17.3 July 2017 floods in South China. 1 in 100 year JRC flood map for South Asia (a) and detail of the Zishui River near Pingkou, Hunan Province (b), showing the probability of ensemble streamflow predictions [%] to exceed a 20 year return period discharge from GloFAS forecasts of June 28th, 2017 (purple shades), the 1 in 100 year JRC flood map (blue shades), and DFO satellite derived SAR image of flooded areas on July 3rd, 2017 (in red).

While inundation models also represent inundation depths and extent for all time steps of the simulations, this is limited by the accuracy of the underlying global DEM (see Schumann et al., 2014; Yamazaki et al., 2017) and by the overestimation of the inundation extent due to the difficulty in including information on local flood protection structures in the inundation model. The latter issue is typically addressed by using global data sets of flood protection standards based on return period estimates (e.g., Scussolini et al., 2016), and assuming inundation only when the predicted flood magnitude is above such level (Alfieri et al., 2017; Ward et al., 2017).

Satellite Imagery

Remote sensing is a reliable way for monitoring flooded areas in a cost-effective manner, thanks to the variety of satellite products available for flood detection since the late 1980s (e.g., Jain et al., 2005; Joyce et al., 2009; Smith, 1997). This includes satellite maps of inundated areas during past severe events. Satellite flood products have the advantage of representing actual observed flooded areas, including the effect of flood protection and of the local orography, and therefore represent more realistic scenarios than most modeling products. On the other hand, satellite-based flood mapping is limited by cloud cover (particularly for optical sensors), flooding in presence of vegetation, and by the satellite revisiting time (see, e.g., Notti et al., 2018). Although these maps provide information only on the inundation extent, water levels can be estimated by intersecting the spatial information with accurate DEMs (Cohen et al., 2017; Hostache et al., 2009; Matgen et al., 2007).

GFP Products The Dartmouth Flood Observatory (DFO) produced and regularly updates the Global Atlas of Floodplains (http://floodobservatory.colorado.edu), an archive of annual maximum flood extent data since 2000, plus additional flood images pre-2000. In regions with discontinuous flood coverage, the data are grouped into a single class with maximum flood extent as recorded by all available satellite images. The archive has quasiglobal coverage between latitudes 60° south and 56° north.

Probabilistic flood mapping, where a pixel in an image is assigned a probability of being wet based on a statistical metric, is not yet available in an operational sense, although first efforts are promising (Giustarini et al., 2015; Neal et al., 2013). Assigning flood exceedance probabilities to pixels in satellite imagary is still a great challenge, given the limited and discontinuous availability of such imagery. Advancement in probabilistic flood mapping is a priority as it addresses user requests of having a better understanding of the uncertainty in current flood mapping methods.

17.2.3. Hydrological Modeling

Hydrological modeling is another important activity in the GFP, as it directly informs decisions by end users. The hydrological response to a rainfall event produces a delay between the rainfall hyetograph and the consequent flood hydrograph downstream, due to soil saturation and routing of surface runoff in and through the river network. When extreme rainfall events are detected by automatic raingauge networks, weather radars, satellite, or combined products, gridded maps of rainfall intensity are used as input to hydrological models that simulate the spatial variability of streamflows and other hydrological variables in the near future, with improved skills in comparison to NWP-driven simulations. The lead-time of skillful forecasts increases with the upstream area of a particular river location, due to the longer delay between the hyetograph centroid and the consequent flood hydrograph.

GFP Products

Within the GFP, the Global Flood Monitoring System (GFMS, http://flood.umd.edu; Wu et al., 2012, 2014) is an experiment funded by the National Aeronautics and Space Administration (NASA) using real-time TRMM Multisatellite Precipitation Analysis (TMPA; where TRMM is the Tropical Rainfall Measuring Mission) and Integrated MultisatellitE Retrievals for GPM (IMERG; where GPM is global precipitation measurement) maps as input to a hydrological model, running on a quasiglobal (50°N–50°S) grid for hydrological runoff and routing simulations. Flood detection and intensity estimates are based on 15 years of retrospective model runs with TMPA input, with flood thresholds derived for each grid location using surface water storage statistics. The GFMS forecast range is 5 days, with observed precipitation fields being extended with short-term forecasts based on NWP the GEOS-5 climate model (Molod et al., 2012).

Similarly, the Floods.Global system (http://floods.global) uses IMERG estimates to produce streamflows and threshold exceedances in the coming 72 h. The IMERG data are available at 0.1° resolution in the range 60°N–60°S, every 30 min, with a 6-h latency. The Ensemble Framework EF5 hydrological model is run at 5-km global resolution every 30 min as new IMERG grids become available.

17.2.4. Monitoring

Flood monitoring is a key part of the disaster response and risk reduction. It focuses on assessing event magnitudes and impacts on the ground, identifying access corridors and supporting emergency operations in the

affected areas. Flood monitoring in nongauged regions is primarily achieved through satellite products based on optical, radar, and passive microwave techniques (Joyce et al., 2009; Smith, 1997; Vörösmarty et al., 1996). Despite the success of optical imagery for flood mapping, persistent cloud cover during floods hampers the systematic application of such imagery, particularly in small to medium-sized basins where floodwaters often recede before weather conditions improve. Given the limitations of sensors operating in the visible and infrared spectrum to acquire flood information routinely, microwave (radar) remote sensing is often considered an attractive alternative or complementary technology for flood detection and monitoring. Microwaves penetrate cloud cover, fog, and light rain, and, in commonly employed radar frequencies, active radar signals from synthetic aperture radar (SAR) are reflected away from the sensor by smooth open water bodies, resulting in a high contrast between the flooded areas compared with dry land.

Multitemporal SAR images have been used successfully to monitor the evolution of a flood event or map inundation dynamics (e.g. Bates et al., 2006; Pulvirenti et al., 2011). In such cases, rapid mapping and dissemination is of course preferable; yet in urban areas, as well as in wetlands and forests, detection of flooding from a SAR image still poses considerable challenges (Schumann & Moller, 2015). In some cases, SAR images acquired over the same area but at different times were used to derive spatially distributed water levels through a complex but powerful technique known as interferometry, or InSAR (e.g., Alsdorf et al., 2000), which will be employed on the upcoming NASA/Centre national d'études spatiales (CNES) Surface Water Ocean Topography (SWOT; http://swot.jpl.nasa.gov; Biancamaria et al., 2016) mission to measure water levels and map water surfaces of the world's lakes and main rivers (Fjørtoft et al., 2014).

In the GFP, flood monitoring connects users, developers, and intermediaries. Also, satellite monitoring can be triggered and improved by early warning systems (Dottori et al., 2017), through earlier and better planning of the acquisition of satellite imagery during emergencies. This interaction is key to improving the range of available flood products that can be produced during extreme events, including complex flooding events in which multiple types of flood occur at the same time.

GFP Products

Satellite-based discharge estimation The River Watch Version 3.4 (http://floodobservatory.colorado.edu/DischargeAccess.html) produces and updates daily a data set of discharge estimates at dozens of gauged and nongauged sites scattered in all continents except Antarctica. It processes microwave radiometry, from existing and previous satellite sensors including TRMM, AMSR-E, AMSR-2, and GPM, to monitor flow area changes due to changes in river width and then link them to discharge through statistical techniques. Below 50° north, data extend continuously back to 1998, while at higher latitudes, data extend only to mid-2002. A global hydrologic model, run for 5 years (2003–2007) with daily time steps is used to calibrate the flow areas to discharge information for nongauged rivers, while sites located on gauged river sections can be calibrated with higher accuracy. The latter is a particularly interesting option to produce real-time and high-quality streamflow information for rivers with stations that are no longer in use or with a long delay in data availability. Van Dijk et al. (2016) analyzed the skills of satellite-based river discharges and found best results ($R > 0.9$) for large and unregulated lowland rivers, particularly in tropical and boreal climate zones. Conversely, generally poor results were obtained in arid and temperate regions.

Satellite-Based Inundation Mapping The Near Real-Time Global Flood Mapping (NRT-GFM) System of NASA's Goddard Space Flight Center (GSFC) produces global daily surface and floodwater maps at approximately 250 m resolution, based on the twice daily overpass of the Moderate-Resolution Imaging Spectroradiometer (MODIS) instrument, on the Terra and Aqua satellites. Surface water is detected by using a ratio of specific bands of the MODIS images, using a technique developed by Brakenridge et al. (2017). Multiday compositing is used to improve the skills of the water detection algorithm, as it is affected by cloud cover and cloud shadows; flooded areas are identified by overlaying the detected water map over a mask of reference water. Various products are generated in 10° × 10° tiles and updated in near real time on the wWorlwide Web (https://floodmap.gsfc.nasa.gov and http://floodobservatory.colorado.edu).

FloodScan (http://product.aer.com/index.php/floodscan) provides daily historical and near-real-time flood maps at 90 m resolution based on satellite microwave sensors (AMSR2, GMI, AMSR-E, and SSM/I), monitoring land areas continent-wide in clear and cloudy conditions from day and night satellite passes. The system derives the flooded fraction at microwave sensor resolution (22–50 km) using an end-member mixing algorithm approach that predicts a local dry land end-member based on historical seasonal variations and recent conditions. The standard product uses a temporal–spatial false positive detection scheme and 3-day averaging to improve accuracy. When the system detects a flooded fraction above background noise levels, it applies a physical downscaling technique to produce higher resolution flood maps based on topography and historical surface water occurrence rates (Pekel et al., 2016). FloodScan covers Africa and North and South America with 1–2 day latency.

17.2.5. Users and Emergency Responders

To maximize the value of the GFP flood products, it is fundamental that:

1. the information reaches decision makers and relevant institutions committed in the emergency management within the affected areas;
2. the products are received in a timely manner, to enable responders to plan and act effectively;
3. the information is communicated clearly, together with confidence levels around the best prediction, or at different probability levels.

One challenge of producing flood information with global coverage is to be able to link to local users from virtually any world region, and to provide them with adequate training so that they understand the products received and their limitations, so they can then take unbiased decisions. For this reason the GFP is engaged with a variety of users, from regional and national hydrometeorological services, to international NGOs and humanitarian organizations, who in turn reach out to the community scale thanks to regional branches and a capillary presence in the field. Among those, the Red Cross Red Crescent Climate Centre adopted the forecast-based financing (FbF; see Coughlan de Perez et al., 2016) in 2015, a mechanism to release humanitarian funding before the flood event starts, based on forecast information, to reduce risks, enhance preparedness and response, and make disaster risk management overall more effective. For example, in 2015, the Red Cross together with the Ugandan Government used GloFAS forecasts to prepare for flooding in the region of Teso in Uganda. Teams distributed water purification tablets, clean water storage containers, and soap to the potentially affected population in advance of the forecasted flood peak, in order to reduce the risk of diarrheal diseases. Since the Ugandan case, FbF has been used operationally in Togo, Bangladesh, and Peru (http://www.climatecentre.org/programmes-engagement/forecast-based-financing), while additional FbF pilots have been established in the Dominican Republic, Haiti, Mozambique, Nepal, Zambia, Mali, Mongolia, Ecuador, and the Philippines.

GFP Products

Another relevant GFP-related activity is the Global Disaster Alert and Coordination System (GDACS; http://www.gdacs.org), a cooperative framework between the United Nations, the European Commission, and disaster managers worldwide to improve alerts, information exchange and coordination in the first phase after major disasters caused by different natural hazards. At present, some 14,000 disaster managers from governmental and nongovernmental organizations can rely on GDACS's alerts and automatic impact estimations to plan international assistance.

17.3. GFP ACTIVATIONS

17.3.1. The South Asia floods in August 2017

In August 2017, heavy and prolonged monsoon rains caused landslides and floods that killed about 1300 people and affected over 45 million people across India, Nepal, and Bangladesh (https://www.unicef.org/infobycountry/media_100719.html and http://erccportal.jrc.ec.europa.eu/Maps/Daily-maps/mapId/2212/xmps/1580). The flooding started in the northeastern part of India, along the Brahmaputra and its tributaries. As the flood wave moved downstream towards Bangladesh, extreme rains continued in a vast area along the Nepal–India border, causing severe flooding in various tributaries of the Ganges River. In Bangladesh, after the devastation of the first monsoon wave in mid-July, a second flood spell started on 12 August affecting a third of the country and 8 million people. The nation's Ministry of Disaster Management and Relief reported that the 2017 floods were the worst in the past four decades.

The GFP community was activated on 7 August, 3 days before the start of the main flooding in the upper Brahmaputra, following a persistent signal of a major upcoming event from the EFI and GloFAS forecasts (see Figure 17.4). Notably, an experimental suite of GloFAS using ECMWF monthly forecasts as input showed that the system predicted potentially severe conditions as early as 28 July 2017, 12–18 days ahead of the flooding along the major rivers (https://www.ecmwf.int/en/about/media-centre/south-asia-floods-put-new-glofas-river-discharge-forecasts-test).

Based on the flood early warning information, a request for pretasking the acquisition of satellite images was sent on 10 August to the Copernicus Emergency Management Service (EMS) in view of a potential activation by authorized users in the affected countries. As new satellite estimates of precipitation became available, regular updates were provided by the GFMS (Figure 17.5), with its flood product at 1/8° and the high resolution (i.e., 1 km) predicted inundation extent. Additional model results based on various global NWP were shared from GloFAS and from the global flood forecasting system developed at Deltares. Results from multiple hydrological models and input precipitation revealed the importance of a multi-model approach to better identify the uncertainties, not only of the predicted flood magnitude but also of the timing of the flood waves, a key parameter to estimate for optimal planning of satellite imagery acquisitions and of emergency operations.

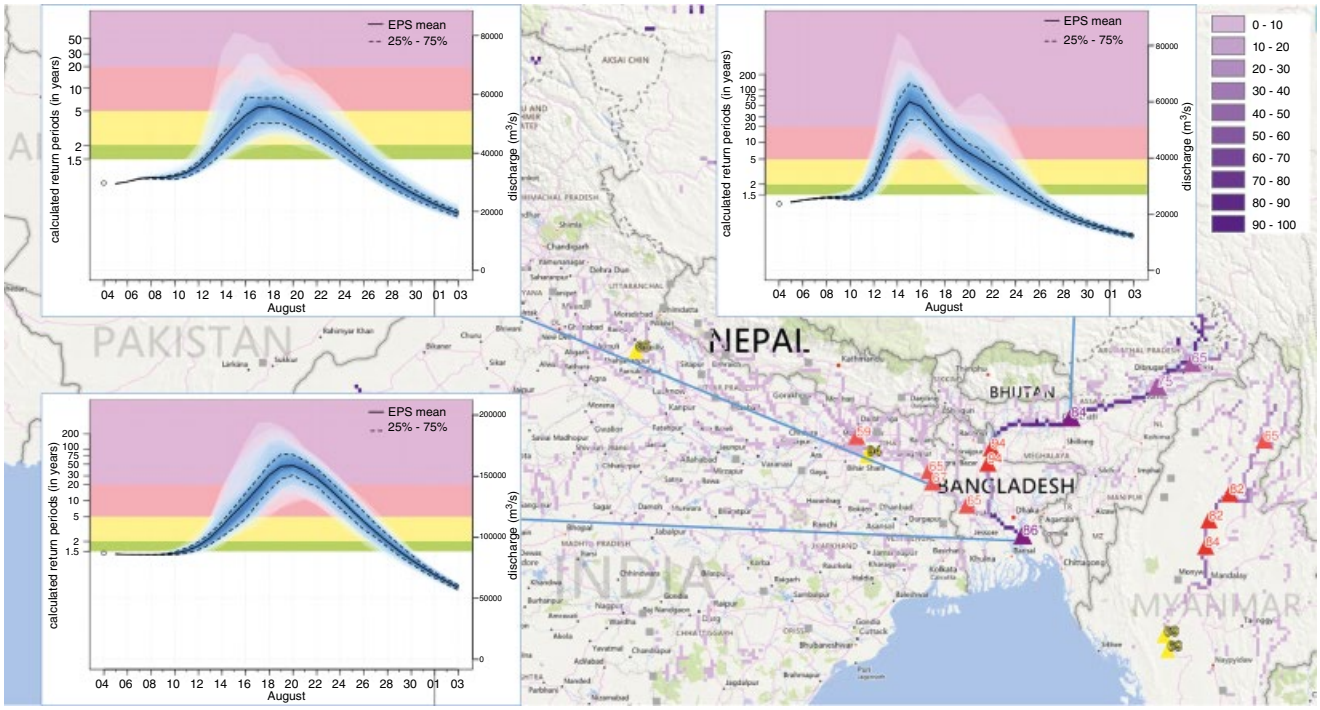

Figure 17.4 Ensemble streamflow predictions from GloFAS forecasts of 4 August 2017, for three reporting points along the Ganges and Brahmaputra rivers. Graphs indicate a high probability of an extreme event from mid-August, with peak flow magnitude up to 1 in 50 year. Purple shades indicate the probability of the ensemble streamflow predictions (%) to exceed a 20 year return period discharge.

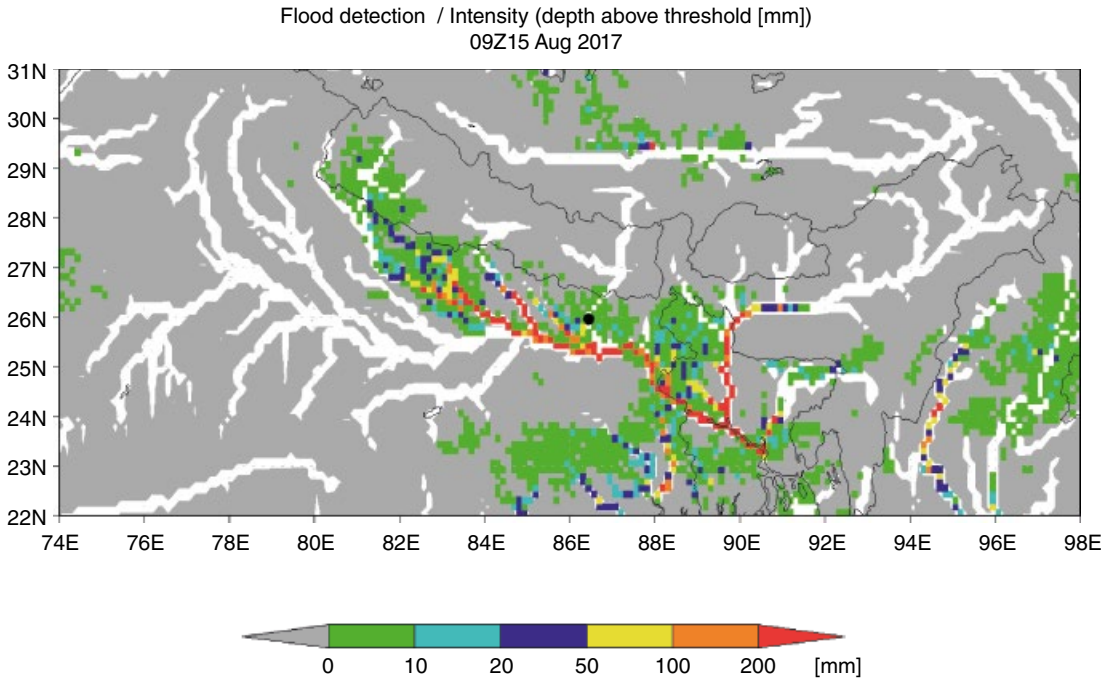

Figure 17.5 The GFMS flood detection estimates over the Ganges–Brahmaputra basin on 15 August 2017.

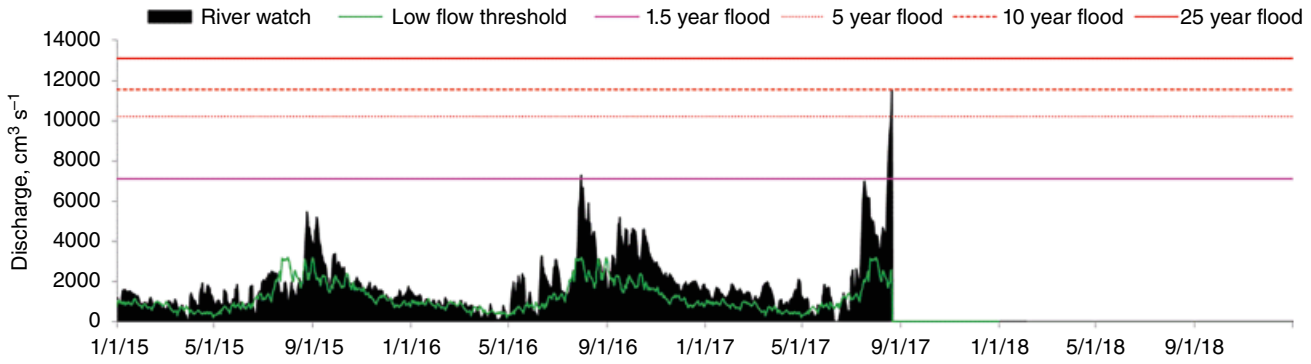

Figure 17.6 Satellite-based river discharge estimates using passive microwave radiometry from River Watch v3.4. Virtual station on the Koshi River, India (see black circle in Figure 17.5) during the August 2017 floods.

Relevant information on the evolution of the flood was available for a number of sites in the River Watch v3.4 database (Figure 17.6), yet with varying skills depending on the location. As floodwaters propagated downstream through the river network, satellite acquisitions enabled a comprehensive spatial coverage of the flood extent and the identification of hotspots of flood risk, through overlay with exposure data such as population density maps, land use, and critical infrastructure. Earliest satellite images made available were from radar and passive microwave sensors (Figure 17.7), due to their capacity to see through the clouds, followed then by optical images.

17.3.2. Hurricane Harvey Flooding in Texas and Louisiana, August–September 2017

Hurricane Harvey made landfall as a category 4 storm at the Texas Gulf Coast (near Rockport) on 25 August 2017, causing wind damage and storm-surge-induced coastal flooding. The storm slowly moved east along the coast (meandering in and out of Gulf waters), in effect, stalling over southeast Texas and southwest Louisiana until 1 September. The slow moving storm produced historically high amounts of rain over the region, with maximum accumulated rainfall of over 1500 mm in southeast Texas. This led to catastrophic riverine and

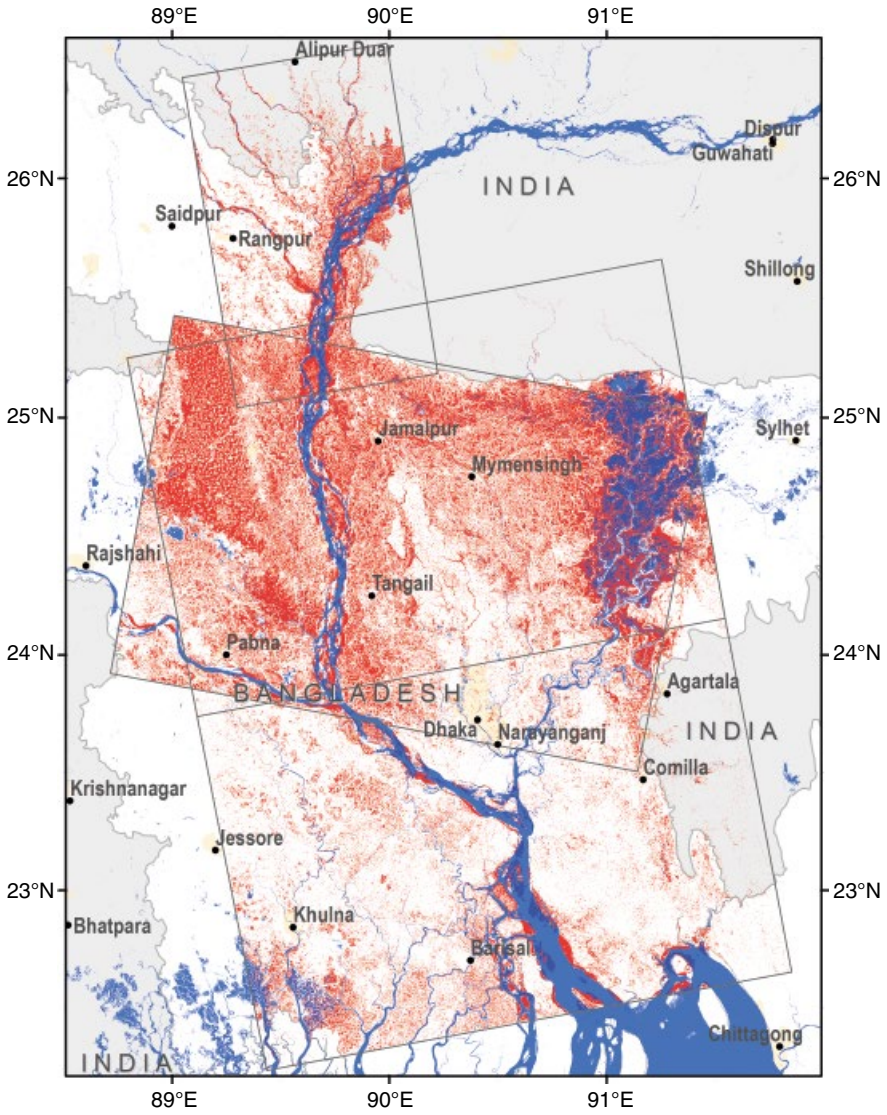

Figure 17.7 Inundation extent (in red) in Bangladesh during the August 2017 flood, based on Sentinel-1 satellite imagery acquired between 15 and 23 August 2017. Surface water with 50% occurrence in 1984–2015 is shown in blue.

flash flooding in the region. Houston Metropolitan area (Texas) received over 750 mm of rainfall between 24 August and 1 September, leading to widespread urban flooding, displacing scores of people and damaging properties and infrastructures. As of 5 September, Moody's Analytics had estimated total damages from Hurricane Harvey at up to $108 billion, ranking it as the costliest natural disaster in United States history (https://www.cnbc.com/2017/09/11/harvey-and-irma-economic-hit-could-total-200-billion-moodys.html).

The GFP is not regularly activated for flooding events in first-world countries, as these typically have established flood prediction and observation capabilities. As a result, GFP activation for this event evolved as its magnitude became apparent. Below we provide a chronology of GFP activities for Hurricane Harvey.

27 August (2 days after landfall)

The DFO sent a limited-distribution email (not via GFP mailing list) providing information about the activation of the "International Charter," the setting up of a DFO event Web page, and available satellite imagery resources from before the flooding. The email led to inclusion of the recipients in the Federal Emergency Management Agency (FEMA) daily Remote Sensing Coordination and Geospatial Coordination calls, which was later proved instrumental in connecting GFP products to the hurricane response community (including for

the following flood events in Florida and Puerto Rico). The email was shared with the National Oceanic and Atmospheric Administration's (NOAA) National Water Center. A few hours following the initial email, precipitation and inundation predictions from the GFMS were shared via the same email distribution.

28 August (flooding in Houston Metropolitan area)

The first email was sent to the GFP mailing list on 28 August, proposing using this event as a case study to test GFP prediction and monitoring systems. The same email also included streamflow predictions from the Flooded Locations And Simulated Hydrographs Project (FLASH; http://blog.nssl.noaa.gov/flash/). These predictions were redistributed to a range of stakeholders (e.g. FEMA, NASA), an action that thereafter became standard operating procedure, with a growing list of recipients.

29 August

The DFO shared (via FEMA Geospatial Coordination email distribution) an update on flood mapping and modeling efforts, including using (nongeoreferenced) Radarsat images (from 28 August) to map flooding, and sharing flood maps from the ALOS-2 satellite produced by NASA's Jet Propulsion Laboratory; confidence in these products was relatively low. Atmospheric and Environmental Research (AER) shared (via the GFP mailing list) a large-scale 90-m resolution flood map of the impacted area, analyzed from the AMSR2 (passive microwave) sensor using an experimental configuration of the FloodScan system. A link between the DFO/GFP and the State Operations Center of the Texas Division of Emergency Management (TDEM) was established, which initiated data sharing on the TDEM (closed to outside users) data server.

30 August

Following an overpass by Sentinel-1 satellite, SAR-based flood maps were shared by Luxembourg Institute of Science and Technology (LIST), JPL, and DFO. The DFO ftp server was used to store and distribute the GIS files of these, and future, products relating to this event. The AER produced an updated maximum flood map for the region using new AMSR2, which was shared via the GFP mailing list. It was then distributed to the FEMA Geospatial Coordination mailing list (over 300 recipients) and was uploaded to the TDEM data server.

31 August

Additional Sentinel-1 imagery was shared by LIST via the GFP mailing list. A request was made by U.S. Geological Survey personnel for further data relating to the AER flood map that was shared the day before. The DFO provided an updated inventory of GFP-produced flood maps and links to its event-dedicated Web-portal and ftp server. The Surface Dynamics Modeling Laboratory (SDML), a GFP partner institute, shared (to FEMA, TDEM, NWC, DFO and AER) a floodwater depth map based on the AER maximum flood extent map. The procedure for compiling such maps was developed in collaboration with the DFO. The AER shared (via the GFP mailing list) updated large-scale maximum flood extent maps incorporating AMSR2 data from 30 August and set up a FloodScan Web interface with daily Hurricane Harvey maps (https://product.aer.com/FloodScan_Harvey). The LIST shared SAR-based flood maps covering the Houston area from a 30 August Sentinel-1 pass. Aerial photography was becoming available via NOAA but with limited coverage outside the coast.

1 September

The AER shared updates from AMSR2 passes on 31 August, revealing the extent of flooding in east Texas (Beaumont area) after the last rain bands moved off to the northeast. The SDML shared a building impact map based on the AER maximum flood extent map and address points layer from the TDEM server (uploaded by University of Texas, Austin). The FEMA personnel requested access to the data for further analysis.

3–5 September

The AER shared final maximum flood extent estimates incorporating all AMSR2 data 26 August to 2 September with expanded coverage into Louisiana (Figure 17.8). The LIST shared flood maps from two Sentinel-1 passes on 4 September.

17.4. DISCUSSION AND CONCLUSIONS

The GFP and its products provide access to a wealth of data focused on flood management, coming from many different groups with a range of different backgrounds. Therefore, a primary challenge is to identify the range of applicability, strengths, and limitations of each product, as well as the complementarity of information from various systems to improve the knowledge on upcoming and ongoing events. Currently, most GFP products are made available through dedicated Web platforms. Here, we call for a single reference portal for operational global flood risk management, where users can see all products in a coordinated manner and receive training on new applications and how to evaluate them. Such an initiative was previously attempted by the JRC with the Global Integrated Flood Map, though it highlighted a number of existing challenges. Here we discuss the main challenges to tackle in order to achieve an

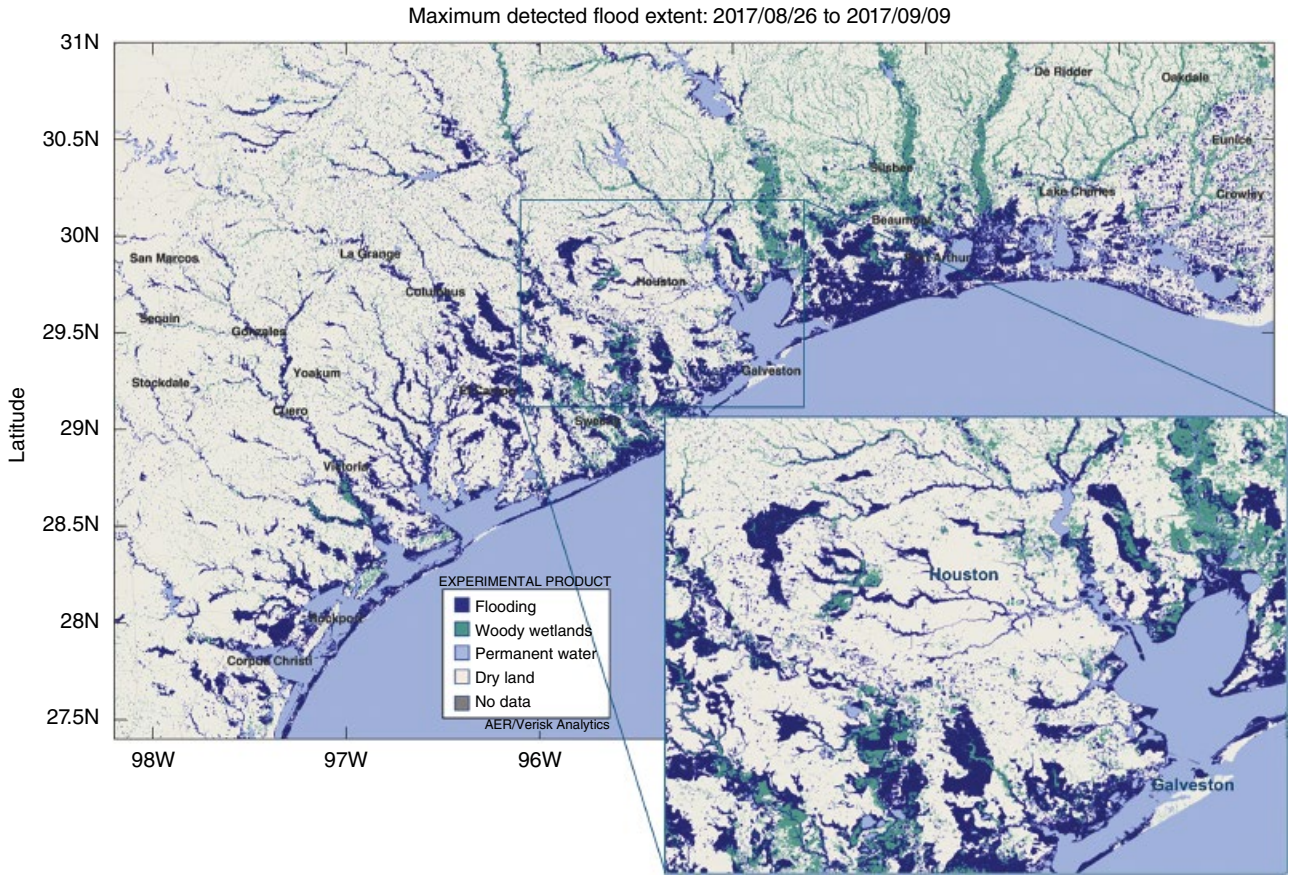

Figure 17.8 Maximum detected flood extent in Texas and Louisiana, USA, following Hurricane Harvey, 26 August to 9 September 2017, from AER's FloodScan algorithm, based on AMSR2 passive microwave remote sensing data downscaled to 90 m resolution. Areas designated as woody wetlands are assumed to be flooded during this event.

effective flood risk management platform, as identified from current and past GFP activities.

• *Time reference and updating frequency*. Most applications are updated on a daily basis, which makes it a suitable time reference for Web visualization. Some systems prove that subdaily updating may provide additional benefits, particularly for short-lived and intense events. Further, experience from EWS has stressed the importance of enabling the data visualization of previous dates, rather than just the latest model output, to enable following the evolution of events and detect persistence or jumpiness of weather forecasts (e.g., Bartholmes et al., 2009).

• *Time validity*. Validity of products may apply to different phases within a flood event. The EWS and hydrological simulations produce output for a range of time steps from the present up to 1 month ahead. Satellite products are often released in near real time, though some composite products include data ranging up to the previous 14 days (e.g., the NRT-GFM), hence their time referencing is less precise. In addition, scenario analysis has no specific indication of time, though it indicates the worst-case scenario for each selected event magnitude. This suggests the need for an additional time dimension referring to the time validity as compared to a selected date t_i, which for current applications would typically range $\{t_i - 15, t_i + 30\}$ days, possibly resorting to multiday aggregation for farther forecast horizons.

• *Spatial resolution*. This varies considerably depending on the product type and is inherently related to the confidence and the timing of each specific output. A clear example is that of Figure 17.3, where EWS show the probability of occurrence of extreme events in the coming 30 days at ~10 km resolution (purple shades), inundation maps at constant magnitude identify the main areas at risk of being inundated at ~1 km resolution, while satellite imagery can detect actual flooded areas during the event at spatial resolution commonly between 10 m (SAR-based, as in Figure 17.3) and 250 m (MODIS-based).

• *Data format and product type*. A key requirement for a common visualization platform is a flexible framework, able to read different data formats and display various types of products including gridded and polygon maps,

time series, and geolocated information, among others. Current back-end and front-end technology can support the integration and comparison of model results for the same event and location.

• *Data upload and download*. Data upload and display must account for products issued at regular intervals (e.g., EWS), as well as on-request products (e.g., satellite flood maps) typically generated once remote sensing data become available. Dialogue with users has pointed out the importance of enabling downloading and printing of custom-made flood products directly from the online platform, coupled with a flexible selection of layers including local exposure, critical infrastructures, and background maps. This raises the issue of sharing data with limited access (e.g., commercial products, restricted user networks) through an open service such as the GFP. Discussion on this topic is still ongoing though solutions are being explored in the sharing of data to selected user groups, or alternatively visualizing derivative products in place of the original input with restricted access (e.g., as for NWP).

• *Interoperability between products and services*. Now in the era of service proliferation, there is an increasing need to make these operate seamlessly with the end-user system in operation. Thus offered products and/or services should be built on open geospatial data standards (such as implemented by the Open Geospatial Consortium (OGC)) that enable full interoperability. In particular, hazard data are most useful if they can be combined with local information on vulnerability and exposure. Hazard data platforms that are interoperable and easily combined with local information are much more likely to be used to prevent major impacts.

• *Performance evaluation*. Quantitative information on product evaluation has been recognized as one of the top priorities for users of flood forecasting and monitoring systems (Wetterhall et al., 2013). Performance evaluation is indeed a key task for systems that integrate and compare products with different input data and skills. The GFP output includes calibrated (e.g., River Watch), non-calibrated (e.g., EFI, NRT-GFM), and mixed systems, where only some specific component is calibrated (e.g., river discharges in some inundation models). Effective interpretation of results should take into account a set of indicators of each system's performance, possibly derived using a common validation data set for all systems. Models producing the same target variable could then be merged by weighting each on their performance, which may vary depending on the geographic location and on the time range, to generate the best overall estimate and the related uncertainty. Providing the recipient with calibrated uncertainty information is critical to enabling use and building trust in model data.

Since the setup of its Web forum in 2011, the GFP has supported operational flood risk management for large-scale flooding worldwide for over 40 independent flood events in six continents. The success of the GFP comes from being part of a global forum with the opportunity to test and improve research tools in real emergency management situations, with huge potential impact on current risk reduction practices over large-scale flood events. Compared to other similar initiatives (e.g., HEPEX (https://hepex.irstea.fr/), WMO HydroSOS (http://www.wmo.int/pages/prog/hwrp/chy/hydrosos/index.php), NASA Disaster Program (https://disasters.nasa.gov/disasters)), the GFP is unique in including all the following three key features: (a) focusing on different phases of the flood risk management cycle, from the early warning to the monitoring and recovery process; (b) a global coverage, particularly important for countries with no or limited alternatives for flood prediction and monitoring; and (c) its operational activities, which couple the development of new techniques with application to upcoming and ongoing flood events.

Being a voluntary and unfunded project, the main activities of GFP members must also meet the objectives of their own research group or project. This has already created a number of collaborations among various GFP partners, which are realized through joint research activities, conference sessions, and new products for operational flood monitoring (De Groeve et al., 2015; Revilla-Romero et al., 2015; Schumann et al., 2016; Trigg et al., 2016; Ward et al., 2015).

We invite more institutes to join the GFP and share their products to support and improve current capabilities in disaster risk management. Research communities active on flash floods, coastal floods, water-related landslides, as well as teams working on estimating surface water elevation through satellite altimetry sensors, are particularly relevant to the GFP for the complementarity of information they provide. Further, we stress the importance of having a global representation of GFP members to ensure a full picture of major events ongoing worldwide, the support of experts from various regions, and direct links to relevant end users at local level, for a prompt and effective communication of flood information and user feedback.

REFERENCES

Adams, T.E., & Pagano, T.C. (2016). *Flood forecasting: A global perspective*. Academic Press.

Alfieri, L., Bisselink, B., Dottori, F., Naumann, G., de Roo, A., Salamon, P., Wyser, K., & Feyen, L. (2017). Global projections of river flood risk in a warmer world. *Earth's Future*, *5*, 171–182. doi:10.1002/2016EF000485

Alfieri, L., Burek, P., Dutra, E., Krzeminski, B., Muraro, D., Thielen, J., & Pappenberger, F. (2013). GloFAS—global ensemble streamflow forecasting and flood early warning. *Hydrology and Earth Systems Science*, *17*, 1161–1175. doi:10.5194/hess-17-1161-2013

Alsdorf, D.E., Melack, J.M., Dunne, T., Mertes, L.A.K., Hess, L.L., & Smith, L.C. (2000). Interferometric radar measurements of water level changes on the Amazon flood plain. *Nature*, *404*, 174. https://doi.org/10.1038/35004560

Alsdorf, D.E., Rodríguez, E., & Lettenmaier, D.P. (2007). Measuring surface water from space. *Reviews in Geophysics*, *45*, RG2002. doi:10.1029/2006RG000197

Bartholmes, J.C., Thielen, J., Ramos, M.H., & Gentilini, S. (2009). The European flood alert system EFAS—Part 2: Statistical skill assessment of probabilistic and deterministic operational forecasts. *Hydrology and Earth Systems Science*, *13*, 141–153.

Bates, P.D., Wilson, M.D., Horritt, M.S., Mason, D.C., Holden, N., & Currie, A. (2006). Reach scale floodplain inundation dynamics observed using airborne synthetic aperture radar imagery: Data analysis and modelling. *Journal of Hydrology*, *328*, 306–318. https://doi.org/10.1016/j.jhydrol.2005.12.028

Bernhofer, M., Whyman, C., Trigg, M.A., Sleigh A., Smith, A., Sampson, C.C., et al. (2018). A first collective validation of global fluvial flood models for major floods in Nigeria and Mozambique. *Environmental Research Letters*, *13*(10), 104007. doi:10.1088/1748-9326/aae014

Biancamaria, S., Lettenmaier, D.P., & Pavelsky, T.M. (2016). The SWOT mission and its capabilities for land hydrology. *Surveys in Geophysics*, *37*, 307–337. doi:10.1007/s10712-015-9346-y

Bouttier, F., & Kelly, G. (2001). Observing-system experiments in the ECMWF 4D-Var data assimilation system. *Quarterly Journal of the Royal Meteorological Society*, *127*, 1469–1488. doi:10.1002/qj.49712757419

Brakenridge, G.R., Anderson, E., Kettner, A.J., Slayback, D., & Policelli, F. (2017). *Current flood conditions*. Dartmouth Flood Observatory. http://floodobservatory.colorado.edu

Calmant, S., Seyler, F., & Cretaux, J.F. (2008). Monitoring continental surface waters by satellite altimetry. *Surveys in Geophysics*, *29*, 247–269. doi:10.1007/s10712-008-9051-1

Cohen, S., Brakenridge, G.R., Kettner, A., Bates, B., Nelson, J., McDonald, R., et al. (2017). Estimating floodwater depths from flood inundation maps and topography. *Journal of the American Water Resources Association*, *54*(4), 847–858. https://doi.org/10.1111/1752-1688.12609

Coughlan de Perez, E., van den Hurk, B., van Aalst, M.K., Amuron, I., Bamanya, D., Hauser, T., et al. (2016). Action-based flood forecasting for triggering humanitarian action. *Hydrology and Earth Systems Science*, *20*, 3549–3560. doi:10.5194/hess-20-3549-2016

De Groeve, T., Thielen-Del Pozo, J., Brakenridgdge, R., Adler, R., Alfieri, L., Kull, D., et al. (2015). Joining forces in a global flood partnership. *Bulletin of the American Meteorological Society*, *96*, ES97–ES100. doi:10.1175/BAMS-D-14-00147.1

Dottori F., Kalas M., Salamon P., Bianchi A., Alfieri L., & Feyen L. (2017). An operational procedure for rapid flood risk assessment in Europe. *Natural Hazards and Earth System Sciences*, *17*(7), 1111–1126.

Dottori, F., Salamon, P., Bianchi, A., Alfieri, L., Hirpa, F.A., & Feyen, L. (2016). Development and evaluation of a framework for global flood hazard mapping. *Advances in Water Resources*, *94*, 87–102. doi:10.1016/j.advwatres.2016.05.002

Emerton, R.E., Stephens, E.M., Pappenberger, F., Pagano, T.C., Weerts, A.H., Wood, A.W., et al. (2016). Continental and global scale flood forecasting systems. *Wiley Interdisciplinary Reviews Water*, *3*, 391–418. https://doi.org/10.1002/wat2.1137

Fjørtoft, R., Gaudin, J.M., Pourthié, N., Lalaurie, J.C., Mallet, A., Nouvel, J.F., et al. (2014). KaRIn on SWOT: Characteristics of near-nadir Ka-band interferometric SAR imagery. *IEEE Transactions on Geoscience and Remote Sensing*, *52*, 2172–2185. https://doi.org/10.1109/TGRS.2013.2258402

Giustarini, L., Chini, M., Hostache, R., Pappenberger, F., & Matgen, P. (2015). Flood hazard mapping combining hydrodynamic modeling and multi annual remote sensing data. *Remote Sensing*, *7*, 14200–14226. doi:10.3390/rs71014200

Hirpa, F.A., Salamon, P., Alfieri, L., Pozo, J.T., Zsoter, E., & Pappenberger, F. (2016). The effect of reference climatology on global flood forecasting. *Journal of Hydrometeorology*, *17*, 1131–1145. doi:10.1175/JHM-D-15-0044.1

Hostache, R., Matgen, P., Schumann, G., Puech, C., Hoffmann, L., & Pfister, L. (2009). Water level estimation and reduction of hydraulic model calibration uncertainties using satellite SAR images of floods. *IEEE Transactions on Geoscience and Remote Sensing*, *47*, 431–441. doi:10.1109/TGRS.2008.2008718

Jain, S.K., Singh, R.D., Jain, M.K., & Lohani, A.K. (2005). Delineation of flood-prone areas using remote sensing techniques. *Water Resources Management*, *19*, 333–347.

Jonkman, S.N. (2005). Global perspectives on loss of human life caused by floods. *Natural Hazards*, *34*, 151–175. doi:10.1007/s11069-004-8891-3

Joyce, K.E., Belliss, S.E., Samsonov, S.V., McNeill, S.J., & Glassey, P.J. (2009). A review of the status of satellite remote sensing and image processing techniques for mapping natural hazards and disasters. *Progress in Physical Geography*, *33*, 183–207. doi:10.1177/0309133309339563

Lalaurette, F. (2003). Early detection of abnormal weather conditions using probabilistic extreme forecast index. *Quarterly Journal of the Royal Meteorological Society*, *129*, 3037–3057.

Matgen, P., Schumann, G., Henry, J.-B., Hoffmann, L., & Pfister, L. (2007). Integration of SAR-derived river inundation areas, high-precision topographic data and a river flow model toward near real-time flood management. *International Journal of Applied Earth Observation and Geoinformation*, *9*, 247–263. doi:10.1016/j.jag.2006.03.003

Molod, A., Takacs, L., Suarez, M., Bacmeister, J., Song, I.-S., & Eichmann, A. (2012). *The GEOS-5 atmospheric general circulation model: Mean climate and development from MERRA to Fortuna*. Greenbelt, MD: NASA Goddard Space Flight Center.

Molteni, F., Buizza, R., Palmer, T.N., & Petroliagis, T. (1996). The ECMWF ensemble prediction system: Methodology and validation. *Quarterly Journal of the Royal Meteorological Society*, *122*, 73–119.

Neal, J., Keef, C., Bates, P., Beven, K., & Leedal, D. (2013). Probabilistic flood risk mapping including spatial dependence. *Hydrological Processes*, *27*, 1349–1363. https://doi.org/10.1002/hyp.9572

Notti, D., Giordan, D., Caló, F., Pepe, A., Zucca, F., & Galve, J.P. (2018). Potential and limitations of open satellite data for flood mapping. *Remote Sensing*, *10*, 1673. https://doi.org/10.3390/rs10111673

Pappenberger, F., Dutra, E., Wetterhall, F., & Cloke, H. (2012). Deriving global flood hazard maps of fluvial floods through a physical model cascade. *Hydrology and Earth Systems Science (Discussion)*, *9*, 6615–6647.

Pekel, J.-F., Cottam, A., Gorelick, N., & Belward, A.S. (2016). High-resolution mapping of global surface water and its long-term changes. *Nature*, *540*, 418–422. doi:10.1038/nature20584

Pesaresi, M., Ehrlich, D., Kemper, T., Siragusa, A., Florczyk, A.J., Freire, S., & Corbane, C. (2017). *Atlas of the human planet 2017: Global exposure to natural hazards (EUR 28556 EN)*. Luxenbourg:Joint Research of the European Union.

Pulvirenti, L., Pierdicca, N., Chini, M., & Guerriero, L. (2011). An algorithm for operational flood mapping from Synthetic Aperture Radar (SAR) data using fuzzy logic. *Natural Hazards and Earth System Science*, *11*, 529–540. https://doi.org/10.5194/nhess-11-529-2011

Raynaud, D., Thielen, J., Salamon, P., Burek, P., Anquetin, S., & Alfieri, L. (2015). A dynamic runoff coefficient to improve flash flood early warning in Europe: Evaluation on the 2013 central European floods in Germany. *Meteorological Applications*, *22*(3), 410–418. doi:10.1002/met.1469, 2015

Revilla-Romero, B., Hirpa, F.A., Pozo, J.T., Salamon, P., Brakenridge, R., Pappenberger, F., & De Groeve, T. (2015). On the use of global flood forecasts and satellite-derived inundation maps for flood monitoring in data-sparse regions. *Remote Sensing*, *7*, 15702–15728. doi:10.3390/rs71115702

Sampson, C., Smith, A., Bates, P., Neal, J., Alfieri, L., & Freer, J. (2015). A high-resolution global flood hazard model. *Water Resources Research*, *51*, 7358–7381. doi:10.1002/2015WR016954

Schumann, G.J.-P., Bates, P.D., Neal, J.C., & Andreadis, K.M. (2014). Technology: Fight floods on a global scale. *Nature*, *507*, 169–169. doi:10.1038/507169e

Schumann, G.J.-P., Frye, S., Wells, G., Adler, R., Brakenridge, R., Bolten, J., et al. (2016). Unlocking the full potential of Earth observation during the 2015 Texas flood disaster. *Water Resources Research*, *52*, 3288–3293. doi:10.1002/2015WR018428

Schumann, G.J.-P., & Moller, D.K. (2015). Microwave remote sensing of flood inundation. *Physics and Chemistry of the Earth, Parts A/B/C*, *83–84*, 84–95. https://doi.org/10.1016/j.pce.2015.05.002

Scussolini, P., Aerts, J.C.J.H., Jongman, B., Bouwer, L.M., Winsemius, H.C., de Moel, H., & Ward, P.J. (2016). FLOPROS: an evolving global database of flood protection standards. *Natural Hazards and Earth System Science*, *16*, 1049–1061. doi:10.5194/nhess-16-1049-2016

Smith, L.C. (1997). Satellite remote sensing of river inundation area, stage, and discharge: a review. *Hydrological Processes*, *11*, 1427–1439. doi:10.1002/(SICI)1099-1085(199708)11:10<1427::AID-HYP473>3.0.CO;2-S

Thielen, J., Bartholmes, J., Ramos, M.-H., & De Roo, A. (2009). The European flood alert system—part 1: Concept and development. *Hydrology and Earth Systems Science*, *13*, 125–140.

Trigg, M.A., Birch, C.E., Neal, J.C., Bates, P.D., Smith, A., Sampson, C.C., et al. (2016). The credibility challenge for global fluvial flood risk analysis. *Environmental Research Letters*, *11*, 094014. doi:10.1088/1748-9326/11/9/094014

UNISDR. (2015). *Making development sustainable, the future of disaster risk management: Global assessment report on disaster risk reduction 2015*. Geneva, Switzerland: United Nations Office for Disaster Risk Reduction.

Van Dijk, A.I.J.M., Brakenridge, G.R., Kettner, A.J., Beck, H.E., De, G., & Schellekens, J. (2016). River gauging at global scale using optical and passive microwave remote sensing. *Water Resources Research*, *52*, 6404–6418. doi:10.1002/2015WR018545

Vörösmarty, C.J., Willmott, C.J., Choudhury, B.J., Schloss, A.L., Stearns, T.K., Robeson, S.M., & Dorman, T.J. (1996). Analyzing the discharge regime of a large tropical river through remote sensing, ground-based climatic data, and modeling. *Water Resources Research*, *32*, 3137–3150. doi:10.1029/96WR01333

Ward, P.J., Jongman, B., Aerts, J.C.J.H., Bates, P.D., Botzen, W.J.W., Diaz Loaiza, A., et al. (2017). A global framework for future costs and benefits of river-flood protection in urban areas. *Nature Climate Change. 7*, 642–646. doi:10.1038/nclimate3350

Ward, P.J., Jongman, B., Salamon, P., Simpson, A., Bates, P., Groeve, T.D., et al. (2015). Usefulness and limitations of global flood risk models. *Nature Climate Change*, *5*, 712–715. doi:10.1038/nclimate2742

Ward, P.J., Jongman, B., Weiland, F.S., Bouwman, A., Beek, R. van, Bierkens, M.F.P., Ligtvoet, W., & Winsemius, H.C. (2013). Assessing flood risk at the global scale: model setup, results, and sensitivity. *Environmental Research Letters*, *8*, 044019. doi:10.1088/1748-9326/8/4/04401

Wetterhall, F., Pappenberger, F., Alfieri, L., Cloke, H.L., Thielen-del Pozo, J., Balabanova, S., et al. (2013). HESS Opinions "Forecaster priorities for improving probabilistic flood forecasts." *Hydrology and Earth System Science*, *17*, 4389–4399. https://doi.org/10.5194/hess-17-4389-2013

Wu, H., Adler, R.F., Hong, Y., Tian, Y., & Policelli, F. (2012). Evaluation of global flood detection using satellite-based rainfall and a hydrologic model. *Journal of Hydrometeorology*, *13*, 1268–1284. doi:10.1175/JHM-D-11-087.1

Wu, H., Adler, R.F., Tian, Y., Huffman, G.J., Li, H., & Wang, J. (2014). Real-time global flood estimation using satellite-based precipitation and a coupled land surface and routing model. *Water Resources Research*, *50*, 2693–2717. doi:10.1002/2013WR014710

Yamazaki, D., Ikeshima, D., Tawatari, R., Yamaguchi, T., O'Loughlin, F., Neal, J.C., et al. (2017). A high-accuracy map of global terrain elevations. *Geophysical Research Letters*, *44*, 5844–5853. doi:10.1002/2017GL072874

Yamazaki, D., Kanae, S., Kim, H., & Oki, T. (2011). A physically based description of floodplain inundation dynamics in a global river routing model. *Water Resources Research*, *47*, W04501.

Zsoter, E. (2006). Recent developments in extreme weather forecasting. *ECMWF Newsletter*, *107*, 8–17.

Zsoter, E., Pappenberger, F., & Richardson, D. (2015). Sensitivity of model climate to sampling configurations and the impact on the Extreme Forecast Index. *Meteorological Applications*, *22*, 236–247. doi:10.1002/met.1447.